Morphology and evolution of VIPERS galaxies

Janusz Krywult[1], Agnieszka Pollo[2,3] and The VIPERS Team[4]

1. Institute of Physics, Jan Kochanowski University, Swietokrzyska 15, Kielce, Poland
2. Astronomical Observatory, Jagiellonian University, Orla 171, Krakow, Poland
3. National Centre for Nuclear Research, Hoza 69, Warszawa, Poland
4. The VIPERS Team coauthors are presented at the end of this proceedings

Using the spectroscopic and photometric data from the VIMOS Public Extragalactic Redshift Survey (VIPERS), together with the CFHTLS T0006 CCD images, we analyze co-evolution of rest-frame colours and Sérsic indices of the early and late-type galaxies in the redshift range $0.5 < z < 1.0$. We find a strong Gaussian bimodality of both the galaxy rest-frame colour and Sérsic index distribution in the redshift – luminosity plane. We propose a new empirical model of galaxy colour and Sérsic index dependence on redshift and luminosity, to study the dynamical and chemical evolution of galaxies.

1 Introduction

Galaxies are observed in the local Universe in various morphological types. The main two broad groups among the large galaxies are spiral and elliptical ones. In the case of more distant objects, measurements of radial luminosity profiles also allow to distinguish betwen disk-like and spheroidal objects. Based on optical colours, galaxies can be classified as blue (star forming) or red (filled with old galaxy population). Locally, the poulation of large galaxies is dominated by two classes of objects: star-forming disk-like galaxies and red quenched elliptical galaxies.

This morphology-color relation is roughly observed at least up to redshift $z \sim 1$ but the shape determination of distant objects is increasingly difficult. The detailed history and mechanisms behind co-evolution of different galaxy properties are still far from clear shich puts properties of intermediate redshift galaxies in the center of interest of extragalactic astrophysics.

In this paper we present measurements of galaxy morphological parameters from the VIPERS (VIMOS Public Extragalactic Redshift Survey)[1] an ongoing ESO large program to map in detail the spatial distribution of $\sim 100,000$ galaxies at redshift $0.5 \leq z \leq 1.2$ and $i_{AB} < 22.5$ (Guzzo et al., 2014). It covers 24 deg^2 on the sky in two fields of the Canada-France Hawaii Telescope Legacy Survey (CFHTLS) and gives an unprecedented possibility to study such a large population of galaxies at these redshifts.

[1]Funding for VIPERS has been provided by the PRIN-INAF 2008 grant "VIMOS Public Extragalactic Redshift Survey (VIPERS): the large scale structure and growth rate of the Universe at $z \sim 1$ from a survey of 100,000 galaxy redshifts." The VIPERS web site is http://www.vipers.inaf.it/. In particular, we acknowledge the support from the National Science Centre (UMO-2012/07/B/ST9/04425 and UMO-2013/09/D/ST9/04030).

2 Data

In this paper we use data from the VIPERS Public Data Release 1 (PDR-1) catalog[2]. We selected galaxies with redshifts estimated with the highest reliability. To model light profiles of galaxies and fit them with Sérsic profiles we applied the GALFIT code (Peng et al., 2002). We used the Terapix T0006 (Goranova et al., 2009) publicly available CCD images in the i-band covering the area observed by the VIPERS. The i photometric band provides a good image quality with a low mean full width at half maximum (FWHM) which is important for the galaxy image decomposition. After rejecting galaxies with poor redshift estimation or image quality, we obtained a sample of 38,507 galaxies. Their absolute B magnitudes (Fritz et al., 2014) were corrected for the evolution of the luminosity function of galaxies, using the Schechter characteristic magnidude B_* in the redshift range $0.05 < z < 2$, computed by Ilbert et al. (2005), which led to the relation:

$$B_* = -21.82 + 2.14 \exp(-2.31z). \tag{1}$$

To study the unbiased sample of galaxies in a possibly large redshift range, we focused our analysis on 24,423 objects in absolute magnitude range $B - B_* = [-1, 1]$.

3 Galaxy colour bimodality

In order to quantify the VIPERS galaxy colour properties we use the $(U - B)$ versus $(B - V)$ colour-colour plot. The distribution shows an evident galaxy colour bimodality of the VIPERS galaxies, with two maxima corresponding to the blue cloud, dominated by late-type galaxies, and the red sequence corresponding to early-type galaxies. We define the UBV rest-frame colour as computed along the line crossing both maxima in the $U - B$ versus $B - V$ galaxy distribution plane.

The galaxy sample was then divided into a grid of five $B - B_*$ luminosity and three redshift bins of the widths equal to 0.5 mag and 0.15, respectively (Krywult et al., 2016). Then, the UBV histograms in each bin were drawn. As shown in Figure 1, the galaxy distribution in each analyzed bin is clearly bimodal and consists of two overlapping normal distributions. The red population dominates at bright luminosities, whereas blue population becomes more visible at fainter magnitudes. A similar picture emerges from the previous studies of local (e.g. Baldry et al., 2004) and intermediate redshift galaxies (e.g. Fritz et al., 2014). From Fig. 1 we can determine the centres of blue and red galaxy histograms as the maxima of the corresponding Gauss functions, marked by the dashed vertical lines in the plot. It can be seen that the centres of both blue and red galaxy histograms are systematically shifted bluewards with the increasing luminosity. At the same time, we observe their shift redwards with the redshift. The dependence of the position of the centres of both galaxy populations in the UBV colour histograms on redshift z and luminosity $B_{corr} = B - B_*$ can be approximated by two–dimensional linear functions:

$$UBV_{\rm r} = 1.606 - 0.282z - 0.065B_{corr}, \tag{2}$$

$$UBV_{\rm b} = 1.180 - 0.426z - 0.185B_{corr}. \tag{3}$$

[2]The first public data release (PDR-1) is available from: http://vipers.inaf.it/rel-pdr1.html

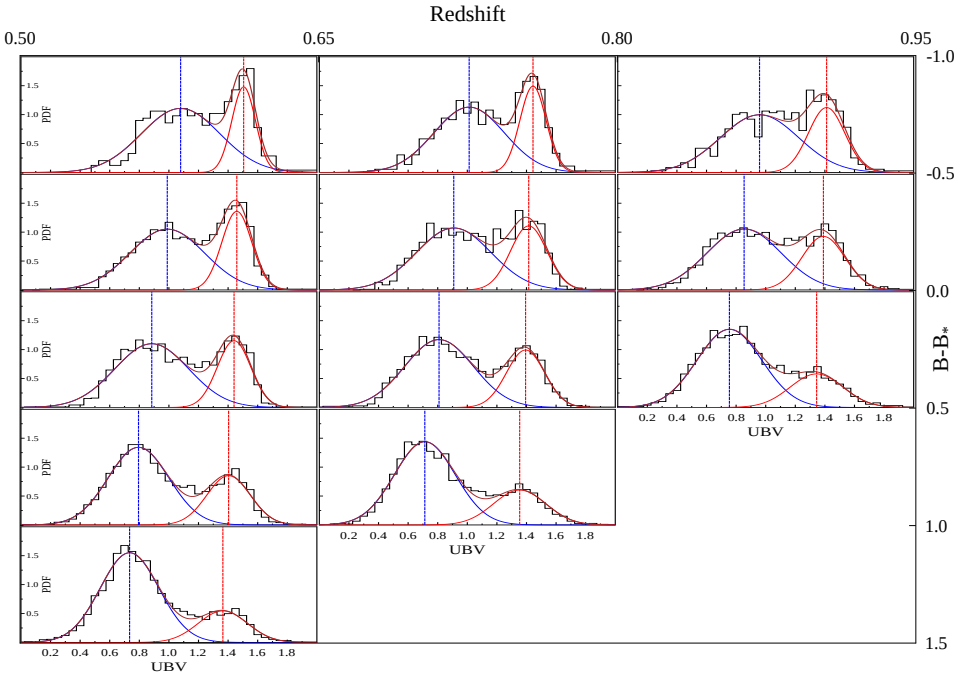

Fig. 1: UBV rest-frame colour histograms in the grid of redshift z and luminosity $B - B_*$ bins. Brown lines represent the simultaneous fit of two Gauss functions, while blue and red lines represent single Gaussian fits to the blue and red galaxy distributions, respectively.

4 Sérsic index bimodality

As the indicator of the galaxy morphology we use the Sérsic index n. We apply the same approach as in the analysis of the UBV rest-frame colour, drawing histograms in the same z and $B - B_*$ bins. We find that in each luminosity and redshift bin the distribution of the Sérsic index n is bimodal. Consequently, we can define two populations: disk-like and spheroidal galaxies. The mean value of n of the VIPERS disk-like galaxies is close to $n = 0.9$, which is a good agreement with a "canonical" value of $n = 1$ of spiral/disk-like galaxies. The mean value of n of the spheroidal population is equal to $n \sim 3.7$, which is only slightly lower than $n = 4$ characterizing de Vaucouleur's profile of local elliptical galaxies. On average, the mean Sérsic index of spheroidal galaxies increases from $n \sim 2$ for fainter objects to $n \approx 4$ for bright galaxies, while n of disk-like galaxies only weakly depends on redshift and luminosity.

We define the "central" values of n for both disk-like and spheroidal population in an analogous way as in the case of the UBV colour, i.e. as the positions of the corresponding maxima of the simultaneously fitted Gaussian functions. Similarly to the case of the UBV colour, the central Sérsic indices of both VIPERS galaxy populations systematically shift both with luminosity and redshift, and their dependence on z and $B_{corr} = B - B_*$ can be well approximated by the linear equations:

$$\log(n_{\rm sph}) = 0.512 - 0.030z - 0.101B_{corr}, \quad (4)$$

$$\log(n_{\rm d}) = 0.048 - 0.118z - 0.074B_{corr}. \quad (5)$$

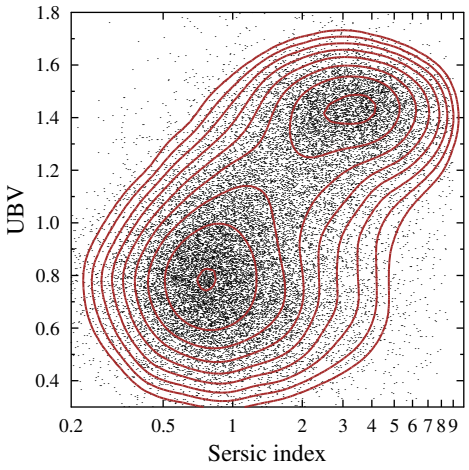

Fig. 2: Sérsic index versus UBV rest-frame colour distribution of the analysed sample of VIPERS galaxies. The contour lines show the galaxy surface density levels separated by 0.15 dex. The bottom left maximum corresponds to the blue/disk-like galaxies, whereas the top right one is dominated by the red/spheroidal objects.

5 Colour–magnitude–morphology relation

The colour-log(n) distribution of VIPERS galaxies (analogous to local Driver et al., 2006, relation) presented in Fig. 2 shows two separate maxima corresponding to the blue/disk-like and red/spheroidal galaxies. To analyse the positions of these maxima as a function of redshift and luminosity we use the relations given by Equations $1 \div 5$, with luminosity and redshift being free parameters changing in the range $z = [0.5, 1.0]$ and $B = [-22.5, -19.5]$, respectively. Solutions to this set of equations are presented in Fig. 3 as the colour-magnitude-morphology (CMM) relation plane. The plot relates four galaxy parameters in one figure which allows for the simultaneous analysis of the evolution of galaxy shapes and colours with redshift as a function of luminosity.

Figure 3 demonstrates that the relation between galaxy morphology and colour changes differently with luminosity and redshift for red/spheroidal and blue/disk-like galaxies. For both types the galaxy UBV rest-frame colour monotonically increases with absolute magnitude B. It implies it is mainly correlated with the speed of the stellar evolution, as young stars located in blue disk-like galaxies evolve faster than old stars forming red spheroidal galaxies. The colour-magnitude relation slope for blue/disk-like galaxies is ~ -0.18 which is in a good agreement with the mean value -0.2 of the Baldry et al. (2004) relation obtained in the same absolute magnitude range for local galaxies. In contrast, the slope of the colour-magnitude relation for red/spheroidal galaxies is less steep, ~ -0.06, which is also close to the locally measured value; for early-type local galaxies Baldry et al. (2004) obtained the slope ~ -0.08, and values reported by other authors vary from -0.1 to -0.04.

It is not yet clear how galaxies evolve from the blue cloud to the red sequence (or move between them). Considered mechanisms include star formation quenching, mergers, gas depletion, or Active Galaxy Nuclei (AGN) feedback. If we take UBV colour as an indicator of the galaxy chemical evolution, we find that for VIPERS disk-like galaxies it proceeds fast, with $UBV \propto -0.43z$. Spheroidal objects evolve more slowly, with $UBV \propto -0.28z$. Moreover, Fig. 3 shows that this process is more efficient for bright (i.e. most likely massive) objects.

Comparison of the top and bottom part of Fig. 3 shows that shapes of galaxies of different populations depend in a different way on redshift and luminosity. The slope of the constant Sérsic index lines shows that the shape of the blue/disk-like galaxies only

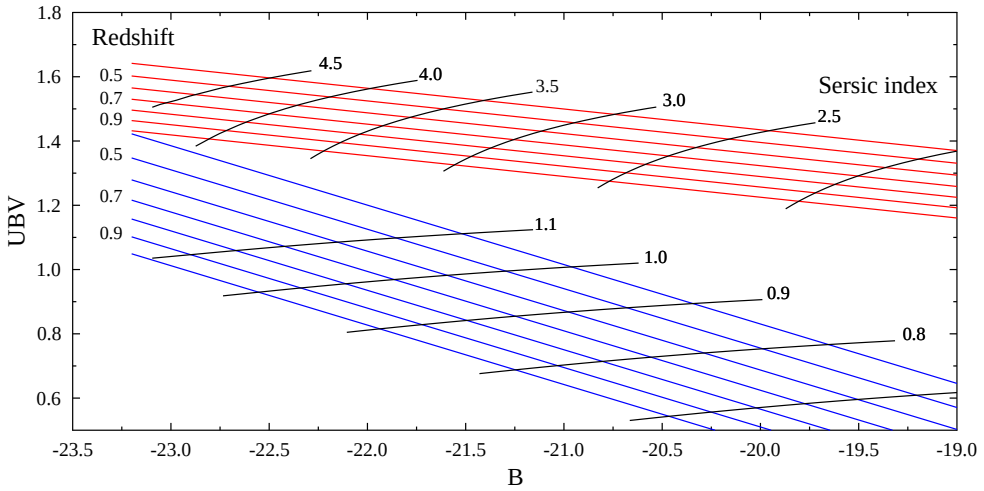

Fig. 3: Colour–magnitude–morphology (CMM) relation for VIPERS galaxies. The blue and red lines show the UBV colour versus absolute magnitude B relation of the red and blue galaxies obtained for the redshift bin indicated on left side of the plot. The black lines and numbers represent constant values of the Sérsic index.

weakly depends on absolute magnitude, $n \propto 10^{-0.07}B$. At the same time, its value slowly increases with cosmic time, as $n \propto (1+z)^{-0.7}$. Using collisionless N body simulations Aguerri et al. (2001) demonstrated that the steepening luminosity profile of disk-like galaxies may be due to satellite accretion, which results in the increase of the Sérsic index of the galaxy bulge by the value proportional to the satellite mass. This process is slower for low mass galaxies, which is consistent with our results.

Red/spheroidal galaxies acquire their shapes fast. Their Sérsic indices increase with cosmic time as $n \propto (1+z)^{-0.5}$, and galaxies became more concentrated. This process can be explained both by accretion and galaxy mergers. Accodrding to (e.g. Buitrago et al., 2013), the formation of giant early-type galaxies through mergers ended around $z \sim 2$. Later massive early-type galaxies grow mainly due to gas accreation, while mergers continue to form smaller ellipticals. The simulations show that this evolutionary difference should result in n of early-type galaxies varying in the range $n = 2 \div 5$ and dependant on the absolute magnitude. Indeed, from our measurements we found that this relation is well described as $n \propto 10^{-0.1}B$. The galaxy is a system which evolves chemically and dynamically and it is impossible to separate both processes, even for well defined blue/disk-like and red/spheroidal populations. Our analysis allows us to relate the rest-frame UBV colour and Sérsic index for these two main galaxy populations. We found that chemical evolution of blue/disk-like galaxies, indicated by their colour, is significantly faster than the dynamical processes shaping their concentrated matter distribution, and the relation between colour and Sérsic index scales as $UBV \propto 2.5n$.

Red/spheroidal galaxies are mainly built by old stars and their chemical evolution is very slow. However, these objects are expected to reshape mass distribution with time. This is in a perfect agreement with our results, as we clearly observe the increase of the Sérsic index with cosmic time. The rest-frame colour dependence of shapes of elliptical galaxies is significantly weaker, with $UBV \propto 0.6n$, than in the case of the disk-like galaxies.

6 Conclusions

We show a strong bimodal distribution of the UBV colour and Sérsic index of the $0.5 < z < 1$ VIPERS galaxies on the redshift–luminosity plane. We quantitatively relate galaxy colours and shapes with their luminosities as a function of redshift. The presented analysis will allow us to trace in detail the evolution the blue/disk-like and red/elliptical galaxies (Krywult et al., 2016).

References

Aguerri, J. A. L., Balcells, M., Peletier, R. F., *Growth of galactic bulges by mergers. I. Dense satellites*, A&A **367**, 428 (2001)

Baldry, I. K., et al., *Quantifying the Bimodal Color-Magnitude Distribution of Galaxies*, ApJ **600**, 681 (2004)

Buitrago, F., Trujillo, I., Conselice, C. J., Häußler, B., *Early-type galaxies have been the predominant morphological class for massive galaxies since only* $z \sim 1$, MNRAS **428**, 1460 (2013)

Driver, S. P., et al., *The Millennium Galaxy Catalogue: morphological classification and bimodality in the colour-concentration plane*, MNRAS **368**, 414 (2006)

Fritz, A., et al., *The VIMOS Public Extragalactic Redshift Survey (VIPERS):. A quiescent formation of massive red-sequence galaxies over the past 9 Gyr*, A&A **563**, A92 (2014)

Goranova, Y., et al., *The CFHTLS T0006 Release*, *http://terapix.iap.fr* (2009)

Guzzo, L., et al., *The VIMOS Public Extragalactic Redshift Survey (VIPERS). An unprecedented view of galaxies and large-scale structure at* $0.5 < z < 1.2$, A&A **566**, A108 (2014)

Ilbert, O., et al., *The VIMOS-VLT deep survey. Evolution of the galaxy luminosity function up to* $z = 2$ *in first epoch data*, A&A **439**, 863 (2005)

Krywult et al., *in preparation* (2016)

Peng, C. Y., Ho, L. C., Impey, C. D., Rix, H.-W., *Detailed Structural Decomposition of Galaxy Images*, *AJ* **124**, 266 (2002)

[1]The VIPERS Team coauthors: U. Abbas[5], C. Adami[4], S. Arnouts[6], J. Bel[7], M. Bolzonella[9], D. Bottini[3], E. Branchini[10·28·29], A. Cappi[9], J. Coupon[12], O. Cucciati[9], I. Davidzon[9·17], G. De Lucia[13], S. de la Torre[14], A. Fritz[3], P. Franzetti[3], M. Fumana[3], B. Garilli[3·4], B. R. Granett[2], L. Guzzo[2·27], O. Ilbert[4], A. Iovino[2], V. Le Brun[4], O. Le Fèvre[4], D. Maccagni[3], K. Małek[16·3], F. Marulli[17·18·9], H. J. McCracken[19], L. Paioro[3], M. Polletta[3], H. Schlagenhaufer[24·20], M. Scodeggio[3], L. A. .M. Tasca[4], R. Tojeiro[11], D. Vergani[25·9], A. Zanichelli[26], A. Burden[11], C. Di Porto[9], A. Marchetti[1·2], C. Marinoni[7], Y. Mellier[19], L. Moscardini[17·18·9], R. C. Nichol[11], J. A. Peacock[14], W. J. Percival[11], S. Phleps[20], M. Wolk[19], G. Zamorani[9] [1] Università degli Studi di Milano; [2] INAF - Osservatorio Astronomico di Brera; [3] INAF - Istituto di Astrofisica Spaziale e Fisica Cosmica Milano; [4] Aix Marseille Université, CNRS, LAM (Laboratoire d'Astrophysique de Marseille); [5] INAF - Osservatorio Astronomico di Torino; [6] Canada-France-Hawaii Telescope; [7] Centre de Physique Théorique, UMR 6207 CNRS-Université de Provence; [8] Université de Lyon; [9] INAF - Osservatorio Astronomico di Bologna; [10] Dipartimento di Matematica e Fisica, Università degli Studi Roma Tre; [11] Institute of Cosmology and Gravitation, Dennis Sciama Building, University of Portsmouth; [12] Institute of Astronomy and Astrophysics, Academia Sinica; [13] INAF - Osservatorio Astronomico di Trieste; [14] SUPA, Institute for Astronomy, University of Edinburgh, Royal Observatory; [16] Department of Particle and Astrophysical Science, Nagoya University; [17] Dipartimento di Fisica e Astronomia - Università di Bologna; [18] INFN, Sezione di Bologna; [19] Institute d'Astrophysique de Paris, UMR7095 CNRS, Université Pierre et Marie Curie; [20] Max-Planck-Institut für Extraterrestrische Physik; [24] Universitätssternwarte München, Ludwig-Maximillians Universität; [25] INAF - Istituto di Astrofisica Spaziale e Fisica Cosmica Bologna; [26] INAF - Istituto di Radioastronomia; [27] Dipartimento di Fisica, Università di Milano-Bicocca; [28] INFN, Sezione di Roma Tre; [29] INAF - Osservatorio Astronomico di Roma